Egyptian Journal of Chemistry

http://ejchem.journals.ekb.eg/

A Green Approach to Produce Low-cost Waste Rubber Tiles Upheld with Recycled Polyethylene and Bagasse

Youssef R. Hassan [1], Ahmed M. Khalil [2, *], Mohamed S. Hasanin [3], Samir Kamel [3]

[1] *Packaging Materials Department, National Research Centre, Dokki 12622, Giza, Egypt*

[2] *Photochemistry Department, National Research Centre, Dokki, Giza 12622, Egypt*

[3] *Cellulose and Paper Department, National Research Centre, Dokki, Giza 12622, Egypt*

Abstract

Recyclability is a key for consumed polymers to diminish their harmful impact on the environment. In this work, reclaimed devulcanized waste rubber (WR), recycled high density polyethylene and bagasse fibers (BF) are used to prepare composites and select from them the optimum one(s) to be applied as low-cost rubber-based tiles. The prepared composites were characterized via gel fraction, mechanical properties including abrasion, hardness, tensile strength and Young's modulus, and thermogravimetric analysis (TGA). Scanning electron microscopy (SEM) was used to study the morphological behavior of the prepared composites, illustrating the impact of loading bagasse fibers to support the properties of these composites. The findings affirm that the RPE and BF were compatible with the reclaimed devulcanized waste rubber. Moreover, the mechanical properties presented acceptable tensile strength values after adding recycled polyethylene (RPE) and BF, whereas the elasticity of the composites was reduced with the addition of fillers. In this context, the hardness and abrasion loss resistance were improved by RPE addition and enhanced more in the presence of BF with maintained thermal stability.

Keywords: Green Tiles; Recycled High Density Polyethylene; Reclaimed Waste Rubber; Bagasse Fibers; Mechanical Properties.

1. Introduction

Through decades, there has been a growing emphasis on sustainability and environmental protection in business and industry [1-3]. This has been driven in part by increasing public awareness of environmental issues, as well as by regulatory pressure and the need to meet corporate social responsibility goals [4-6]. As a result, many organizations are now looking for ways to reduce their environmental impact and increase the use of sustainable materials [7-9]. However, synthetic polymers are used in many domains according to their features as well as the economic dimension. Accordingly, the majority of the synthetic polymers are non-biodegradable ones. This burden could be loaded onto the environment with being accumulated. Polymeric wastes are increasing daily due to the contribution of polymers in numerous applications and apparatuses [10,11]. Many tons of plastic garbage are thought to have been dumped in landfills around the world. This junk offers a significant chance to recover resources through improved landfill mining, which aligns with current efforts to promote the circular economy [12]. Recycling and reclaiming polymers are promising pathways to decrease their environmental hazards. Polyethylene (PE) has the simplest basic structure of low-cost plastic, with different kinds comprising low and high-density PE. It has outstanding electrical insulation properties throughout a broad frequency range, high chemical resistance, superior interaction, and toughness, alongside being a flexible polymer [13]. Degradation of PE in the environment is complex and could take several years.

Worn-out rubber accumulates after being used in tires and other applications. End-of-life tires are a significant global waste problem due to their bulky nature, high durability, and limited recycling options. Waste tires are those materials that have reached the end of their useful life and are discarded as waste. The inability of tires to flow, or deform under pressure, makes them difficult to process through traditional

*Corresponding author e-mail: akhalil75@yahoo.com. (Ahmed M. Khalil)

Received date 06 July 2024; revised date 30 July 2024; accepted date 11 August 2024

DOI: 10.21608/ejchem.2024.302068.9962

reclaiming methods [14-16]. Moreover, agro-wastes are assembled in the environment with the ability to decompose naturally in the environment. Bagasse fibers waste could be employed in many applications comprising being a biodegradable filler [17]. Bagasse fibers are composed of cellulose(s) and lignin. They can be easily integrated into some structures as fillers to improve their physico-mechanical and biodegradability properties [18]. Polymer composites are assorted as polymer matrices reinforced with secondary phases, typically fibers or particles. These composites can show improved properties over those of individual polymers [19-21]. Traditionally, the reinforcement phase has been formulated from virgin materials. However, there is a growing interest in using recycled substrates as more sustainable and eco-friendly alternative materials. The generation and disposal of plastic waste is a significant global environmental concern, with millions of tons of plastic waste [22,23].

The aim of this work is to develop a green recyclability approach via utilizing polymeric composites based on the highest possible amount of WR and RPE with/without BF. The mechanical, morphological and thermal properties of the formulated composites were tested to explore the optimum ones for manufacturing low-cost and ecofriendly green tiles. They are expected to be suitable for industrial applications, particularly as flooring green tiles according to their evaluated properties after being tested.

2. Materials and methods

2.1. Materials

Bagasse fibers (BF) were provided from Quena Paper Industry Company, Egypt. Waste rubber (WR) was provided from the local market, Cairo, Egypt. It is collected from the tread and sidewalls of vehicles tires and then ground. Recycled high density polyethylene was delivered from Al-Amal Co., Egypt. All chemicals and reagents used in this work were purchased from Loba Chem., India, in analytical grade without purification.

The particle size of waste tire powder (WTP) was determined through sieve analysis technique, and the diameter was classified as shown in Table 1 (for 100 g.), the main WTP particle size ranged between 300 and 425 microns.

Table 1. Particle size distribution of WTP (100 g.).

Micron	850	600	425	300	80	<60
WTP (g)	0.5	10	35	44	05	4.6

The chemical analysis of bagasse is 45-55, 20-25, 28, 20, 5 and 2% as cellulose, hemicelluloses, pentosane, lignin, sugar and other minerals, respectively. The bagasse powder was characterized to demonstrate its particle size. Upon investigation through sieve analysis technique, it was found that the diameter of the bagasse powder was classified as shown in Table 2 (for 100 g.), the main BF particle size ranged between 425 and 850 microns.

Table 2. Particle size distribution of bagasse fiber (for 100 g.).

Micron	850	600	425	300	80	<60
BF (g)	19.3	30.0	20.5	13.0	12.8	4.01

2.2. Samples preparation

The composites were prepared according to Table 3. Waste tire rubber was subjected to a thermo-mechanical devulcanization process on a roll mill for 30 min. producing reclaimed devulcanized waste rubber (WR). RPE was introduced to WR on the mill for 5 min., followed by loading bagasse with continuous milling for an extra 5 min. For each sample, sulfur was used to vulcanize the used rubber. Maleic anhydride (MA), was used as a coupling agent. The composites were pressed at 165 ˚C for 15 min forming the required tiles.

Table 3. Composition of the prepared waste rubber-based composites.

Sample	**WR (phr)**	**RPE (phr)**	**Sample**	**WR (phr)**	**RPE (phr)**	**BF (phr)**
E1	100	00				
E2	90	10	E7	90	7	3
E3	80	20	E8	80	14	6
E4	70	30	E9	70	21	9
E5	60	40	E10	60	28	12
E6	50	50	E11	50	35	15

2.3. Characterization

The gel fraction of the insoluble rubber fraction in the samples was defined according to Eq. 1. Subsequently, the tested composites were swelled in toluene and then extracted 72 h later to get rid of any unreacted components or small fragments. The samples were dried at 80 ˚C and reweighed [24].

$$\boldsymbol{Gel\ fraction}\ (\%) = \frac{m_s}{m_i} \times \mathbf{100} \qquad \textbf{Eq. 1}$$

where m_s and m_i are the weight of the dried samples after extraction and before extraction, respectively.

Mechanical properties including tensile strength and Young's modulus were determined by using an Instron 34SC-5 universal tensile testing machine, UK,

equipped with a load cell of 5 kN and a crosshead speed of 10 mm.min-1, according to ASTM D 882-18. The dumbbell specimens were die-cut from the composites. The average of three parallel trails for each sheet was recorded. Hardness was carried out using shore A, Harteprufgerate, DIN 53505, ASTM 2240. The abrasion was tested using Taber Rotary Abrasion 5150, abrading wheel H-22, auxiliary weight 500 g load for 1000 cycles.

The dynamic mechanical properties were evaluated through the dynamic mechanical analyzer DMA1 (Mettler Toledo, Switzerland). The measurements were carried out to assess the different dynamic-mechanical moduli of the tested samples. A single cantilever mode was employed. The samples were subjected to a cyclic shear with a force amplitude of 0.1 N at 1 Hz frequency. Storage modulus (E'), loss (E'') and loss factor (tan δ) were obtained in the temperature range of -20 to 120 ºC with a heating rate of 5 ºC/min.

Scanning electron microscopy (SEM) (JSM 6360LV, EOL/Noran) was used to examine the surface morphology of the prepared composites. SEM images were processed using the free software ImageJ.

TGA analysis was performed on samples using a Perkin Elmer thermogravimetric analyzer by heating the sample to 600 °C at a rate of 10 °C/min under N_2 atmosphere.

3. Results and Discussion

The gel fraction % of WR compared with other prepared composites is illustrated in Fig. 1. The WR sample represented a gel fraction of about 85%. This behavior can be correlated to the interconnected structure resulting from a network formed during the polymerization or crosslinking process. In addition, RPE gradually increased the gel fraction percentage upon increasing the RPE content to reach 95% in composite E6. On the other hand, the BF addition has contributed in elevating the gel fraction in comparison with the WR to 89.7% in E7; to reach 99% in E11. These observations may refer to the present interaction between the composites ingredients.

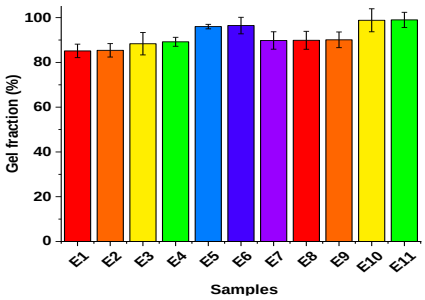

Fig. 1. Gel fraction of the prepared composites.

Fig. 2 shows the tensile strength (TS) of the formulated composites. WR exhibited a low tensile strength of 1.26 MPa. It increased upon inserting RPE into the elastomeric matrix of WR. The inclusion of RPE led to a gradual increase in tensile stress. It reached approximately 10.21 MPa at 50% RPE content (E6). Similarly, introducing of BF gradually decreased the tensile strength with a recorded value of 2.2 MPa in E7. In the context provided, E10 exhibited the highest value of 6.84 MPa compared to all other composites containing BF. The addition of RPE decreased the tensile strength of WR. Then, some signs of recovery have been noticed upon reaching 40% RPE content. Interestingly, the addition of BF generally led to a decrease in tensile strength, excluding the result of E10. This observation could be attributed to the compatibility between the different materials during the blending process. It can be assumed that a well-matched combination resulted in superior mechanical properties. This feature leads to a favorable interface adhesion under critical conditions. Consequently, the results indicate that the interplay between RPE, BF and WR influences the tensile strength behavior of the composite materials. The highest recorded value for E10 suggests a synergistic effect between the components. It led to an enhanced mechanical performance. The decrease in tensile strength with the loading of BF highlights the importance of material selection and compatibility in tiles composites design. These findings underscore the significance of understanding material interactions and compatibility when designing green tile composite materials for specific applications. By optimizing the composition and proportions of different components, it is possible to tailor the mechanical properties of composites to meet desired performance criteria.

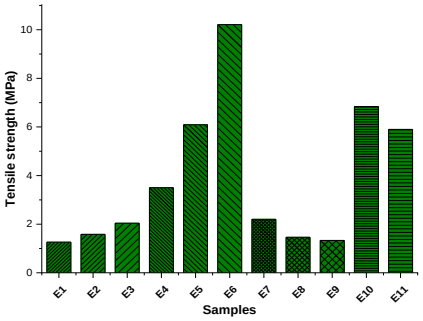

Fig. 2. Tensile strength of WR-based tiles.

It is known that the increase of Young's modulus is an indication of low elasticity [24]. Herein, Fig. 3 displayed the Young's modulus of the prepared tiles. E1 exhibited the lowest Young's modulus value for sole devulcanized waste rubber among the investigated samples. The introduction of RPE reduced the elasticity where Young's modulus increased gradually to reach 763 MPa with E6 having the highest RPE content, which aligned well with the

tensile strength findings. Additionally, incorporating BF also decreased the elasticity with a low impact compared with that of RPE. Whereas, E11 recorded 402 MPa. These observations highlight the interconnection between the tiles composites components. They underscore the significant impact of these reused materials on various mechanical properties assessments.

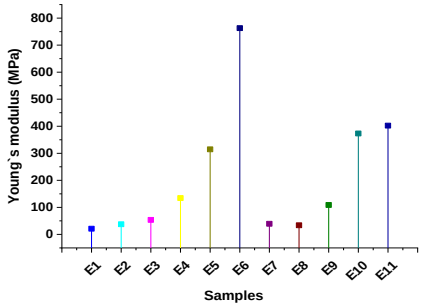

Fig. 3. Young's modulus of WR-based composites.

Fig. 4 shows the hardness of the investigated composites. The data indicate that RPE has a considerable impact on the hardness property. In E6, it is noticed that the hardness value is around 97 N/mm^2 for the composites loaded with 50 phr RPE with 60% more than the value of the blank reclaimed waste rubber (E1). Besides, adding BF affected the hardness significantly compared to RPE. For the tiles with the lowest BF content; tile E7, showed a hardness value of 83 N/mm^2, while that with the highest BF content (E11) recorded 96 N/mm2. In this manner, the high-content RPE composites were offered to improve hardness values compared to blank WR. In addition, BF can be considered good compatible filler in the prepared tiles. The hardness values have been maintained in the composites loaded with BF compared to the other tiles lacking these cellulosic fibers.

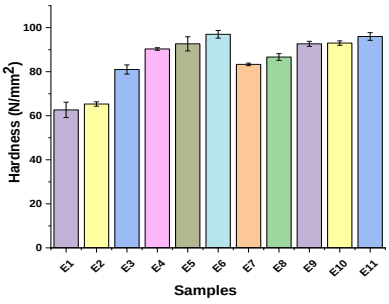

Fig. 4. The hardness of WR-based composites.

In a harmony of abrasion resistance, the addition effect of RPE and BF is represented in Fig. 5. The RPE addition has augmented the resistance to abrasion by about 3 times in E6 (the highest concentration of RPE) in comparison with E1 (blank WR). However, the BF has more abrasion resistance than neat RPE. The presence of BF has enhanced this property due to the compact strength of the fibers that admittedly resist abrasion loss [25]. These suggestions could be supported by the recorded value of E11, with the lowest value of abrasion loss among all samples (30.4 mg) according to the highest concentration of BF. Consequently, loading the plastic and cellulosic contents into the WR matrix significantly influenced the abrasion resistance.

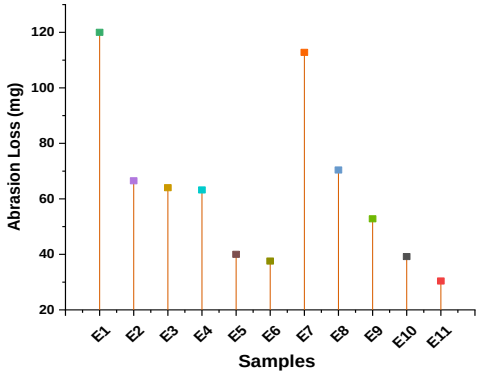

Fig. 5. The abrasion loss of WR-based composites.

The prepared green tiles did not show any physical difference in their appearance as the black tint of the used waste rubber was dominating. It hindered the colour of BF and RPE as shown in Fig. 6.

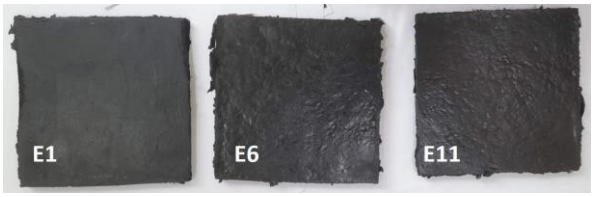

Fig. 6. A digital photo for the prepared tiles.

The morphological investigation of the prepared composites was carried out using SEM with two different magnifications to understand the intermolecular structure of the formulations. E1 (blank WR), E6 (WR and RPE with highest ratio), and E11 (WR, RPE and BF with highest ratio) are presented in Fig. 7. In E1, a cracked surface is observed with a rough texture at the low magnification image (Fig. 7a). The high-magnification image (Fig. 7b) clearly presents the surface details with a layered structure. It consists of many layers sorted up to each other with different sizes, and this is in a good agreement with the literature [26,27]. In addition, E6 in the low magnification image was displayed in a similar structure of black WR stuffed with some filler-like

melted polymer due to the presence of RPE (Fig.7c). Furthermore, the high-magnification image explored the interaction between the WR and RPE with a rough surface appearance (Fig. 7d). Furthermore, the addition of BF was investigated in low and high magnification SEM images as in Fig. 7e and 7f, respectively. They emphasized that they comprise different phases. The surface of E11 performed more smoothness in comparison with the E6. Indeed, these finding were in a nice agreement with the gel fraction findings as well as proving the mechanical characteristics of these composites.

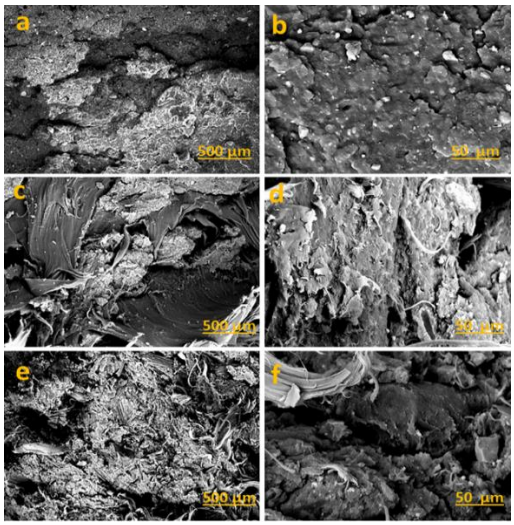

Fig. 7. SEM images of WR-based composites: dWR (E1) with low magnification (a) and high magnification (b). E6 with low magnification (c) and high magnification (d). E11 with low magnification (e) and high magnification (f).

The dynamic mechanical analysis (DMA) of devulcanized waste rubber and its composites with RPE are shown in Fig. 8. When elevating the temperature, the storage and loss moduli of WR and its composites showed decrements in these values, as shown in Fig. 8 (a and b). These dynamic properties pass through various regions when boosting the temperatures. A glassy stage possessing high storage (E') and loss (E") moduli. Such behavior can be referred to as the limited mobility of the elastomeric chains. After that, a transition region displaying a modulus decline can be observed. It indicates the transfer from a glassy state to a rubbery one. The following elastomeric rubbery area showed low moduli values. It refers to the change in the spent energy with high mobility of the reclaimed rubber chains [28]. Loading RPE into WR increased E' and E" values. They show more rigid polymeric chains than sole waste rubber. The introduction of BF decreased the stiffness of elastomeric chains and played a role in reducing the relevant segmental motion and stress relaxation properties of these tiles [29]. BF displayed a good interaction with WR and RPE. It is noticed in Fig. 8c that WR/RPE 50:50 composites showed the lowest tan delta values when compared to the other samples. This feature suggests a fine distribution of these cellulosic fibers in the elastomeric matrix.

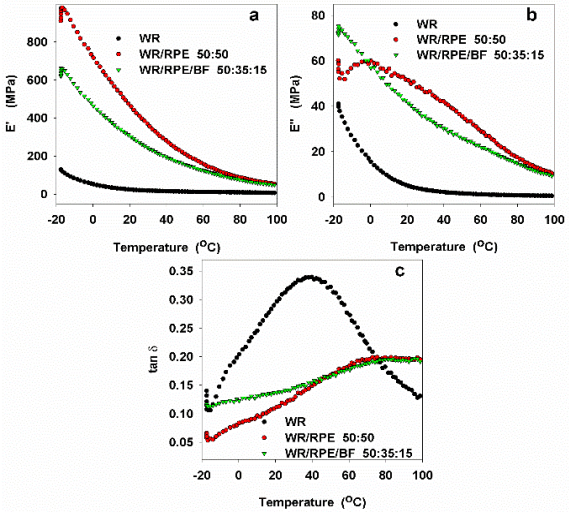

Fig. 8. DMA: (a) Storage, (b) loss moduli and (c) tan delta vs. temperature of WR-based composites.

The thermogravimetric analysis (TGA) technique was followed to monitor the changes in the thermal stability of the prepared samples. Fig. 9a represents the thermal decomposition of waste rubber-based composites. Below 285 °C, a low weight loss % is observed. There is a notable decrement in weight, taking place around 305 °C. Hereby, the organic fragments in tested waste rubber samples degrade at elevated temperatures. Upon comparing WR with the other composites loaded with RPE and BF, it can be noticed that E6 exhibits a higher thermal stability than WR. This behavior elucidates the interaction between the elastomeric chains of WR and those of RPE. It assumes an interfacial adhesion between the present polymeric species with maintained thermal stability [30,31]. Further weight loss arises at higher temperatures due to liberating unstable chemical components. Above 420 °C, degradation of amorphous RPE and rubber chains occurs. As BF was introduced, a slight decrease in thermal stability arose owing to the existence of these cellulosic fibers. Cellulosic substrates decompose through several steps. Hemicellulose decomposes at less than 330 °C. Lignin shows thermal degradation above 500 °C. Fig. 9b illustrates the derivative curves of the investigated composites as a function of temperature. The peaks in the differential curves coincide with mass conversion. WR shows various peaks with a wide thermal decomposition range due to the multicomponent structure in waste rubber. It comprises inorganic fillers alongside carbon black. RPE elucidated a shifted peak from that of WR. BF did not show considerable

variations in TGA values after loading to WR/RPE composites. Furthermore, a breakdown in C-C bonds, hollow cellulose and volatiles in bagasse occurs. Thermal decomposition continues while raising the temperature till bagasse is fully decomposed.

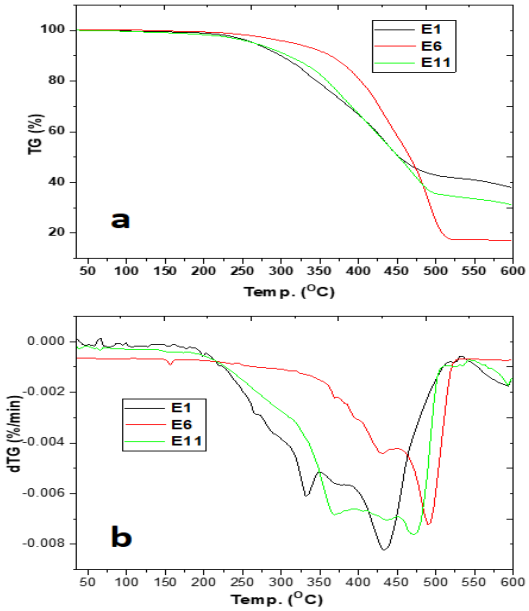

Fig. 9. (a) TGA and (b) dTG thermograms of waste rubber-based composites.

4. Conclusion

In the present study, green tiles based on all waste polymers, reclaimed devulcanized waste rubber, recycled high density polyethylene, and bagasse fibers were successfully prepared.A gel fraction study confirmed the compatibility between the components. Adding recycled polyethylene increased the tensile strength, thermal stability, E' and E'' and reduced the elasticity. Adding bagasse fibers improved the hardness and abrasion loss but did not affect the elasticity. Waste rubber/recycled polyethylene 50:50 and Waste rubber/recycled high polyethylene/bagasse fibers 50:35:15, two created composites, performed well enough to be used as the intended flooring green tiles. Consequently, reusing these waste polymers provides a sustainable solution for reducing the pollution caused by rubber tires and agricultural wastes.

5. Conflicts of interest

There are no conflicts to declare.

6. Funding

This work is funded by Science, Technology & Innovation Funding Authority (STDF) - Egypt.

7. Acknowledgments

This paper is based upon work supported by Science, Technology & Innovation Funding Authority (STDF) under grant number 47192.

8. References

1. Abouzeid, R.; Kamel, S.; Ali, K.A. Microcrystalline cellulose production from sugarcane bagasse as sustainable process: A pilot plant. Egyptian Journal of Chemistry, 2024, 67(9), 35-43.
2. Elsakka, E.A.; Fouad, H.; Hassanin, A. The Use of sawdust and sugarcane bagasse as low cost adsorbent in wastewater treatment. Egyptian Journal of Chemistry 2024, 67(3), 117-125.
3. Hasanin, M.S.; Abd El-Aziz, M.E.; El-Nagar, I.; Hassan, Y.R.; Youssef, A.M. Green enhancement of wood plastic composite based on agriculture wastes compatibility via fungal enzymes. Scientific Reports 2022, 12, 19197.
4. Khalil, A.M.; El-Nemr, K.F.; Hassan, M.L. Acrylate-modified gamma-irradiated olive stones waste as a filler for acrylonitrile butadiene rubber/devulcanized rubber composites. Journal of Polymer Research 2019, 26, 249.
5. El-Saied, H.; Basta, A.H.; Hassanen, M.E.; Korte, H.; Helal, A. Behaviour of rice-byproducts and optimizing the conditions for production of high performance natural fiber polymer composites. Journal of Polymers and the Environment 2012, 20, 838-847.
6. Elleboudy, A.A.F.; Elagoz, M.A.; Simonian, G.N.; Hasanin, M. Biological factors affecting the durability, usability and chemical composition of paper banknotes in global circulation. Egyptian Journal of Chemistry 2021, 64, 2337-2342.
7. Leclerc, S.H.; Badami, M.G. Material circularity in large organizations: Action-research to shift information technology (IT) material flows. Journal of Cleaner Production 2022, 348, 131333.
8. Mehrzad, S.; Taban, E.; Soltani, P.; Samaei, S.E.; Khavanin, A. Sugarcane bagasse waste fibers as novel thermal insulation and sound-absorbing materials for application in sustainable buildings. Building and Environment 2022, 211, 108753.
9. Wiśniewska, P.; Wójcik, N.A.; Ryl, J.; Bogdanowicz, R.; Vahabi, H.; Formela, K.; Saeb, M.R. Rubber wastes recycling for developing advanced polymer composites: A warm handshake with sustainability. Journal of Cleaner Production 2023, 427, 139010.
10. Lazaro-Romero, A.; Contreras-Ramos, S.M.; Dehonor-Gómez, M.; Rojas-García, J.M.; Amaya-Delgado, L. Optimizing cellulose fraction for enhanced utility: Comparative pre-treatment of Agave tequilana Weber var. blue bagasse fiber

for sustainable applications. Heliyon, 2024, 10, 24) e29149.
11. Pan, D.; Su, F.; Liu, C.; Guo, Z. Research progress for plastic waste management and manufacture of value-added products. Advanced Composites and Hybrid Materials 2020, 3, 443-461.
12. Canopoli, L.; Coulon, F.; Wagland, S.T. Degradation of excavated polyethylene and polypropylene waste from landfill. Science of The Total Environment 2020, 698, 134125.
13. Saleh, H.M.; Khalil, A.M. Plastic films based on waste expanded polystyrene loaded with bagasse powder for packaging applications. Egyptian Journal of Chemistry 2022, 65(11), 323-329.
14. Moharir, R.V.; Kumar, S. Challenges associated with plastic waste disposal and allied microbial routes for its effective degradation: A comprehensive review. Journal of Cleaner Production 2019, 208, 65-76.
15. Ferdous, W.; Manalo, A.; Siddique, R.; Mendis, P.; Zhuge, Y.; Wong, H.S.; Lokuge, W.; Aravinthan, T.; Schubel, P. Recycling of landfill wastes (tyres, plastics and glass) in construction–A review on global waste generation, performance, application and future opportunities. Resources, Conservation and Recycling 2021, 173, 105745.
16. Zeid, M.A.; Rabie, S.T.; Nada, A.A.; Khalil, A.M.; Hilal, R.H. Effect of gamma and UV radiation on properties of EPDM/GTR/HDPE blends. Polymer-Plastics Technology and Engineering 2008, 47(6), 567-575.
17. Ilyas, R.; Sapuan, S.; Asyraf, M.; Atikah, M.; Ibrahim, R.; Dele-Afolabi, T.; Hazrol, M. Introduction to biofiller-reinforced degradable polymer composites. In Biofiller-reinforced biodegradable polymer composites; CRC press: 2020; 1-23.
18. Syuhada, D.; Azura, A. Waste natural polymers as potential fillers for biodegradable latex-based composites: A review. Polymers 2021, 13, 3600.
19. Farag, M.M.; Abdelraof, M.; Ahmed, H.Y.; Hasanin, M.S. Comparative study of Mg-phosphate/cellulose and struvite/cellulose composites: Green synthesis, degradation, and biocompatibility. Bioactive Carbohydrates and Dietary Fibre 2022, 28, 100337.
20. Dacrory, S.; Kader, A.H.A.; Hasanin, M.; Kamel, S. Evaluation of biocompatible amino acid-functionalized cellulose composites: Characterizations, molecular modeling, anticoagulant activity, and cytocompatibility. Bioactive Carbohydrates and Dietary Fibre 2023, 30, 100372.
21. Essawy, H.A.; Tawfik, M.E.; Khalil, A.M.; El-Sabbagh, S.H. 2014. Systematic organophilization of montmorillonite: The impact thereof on the rheometric and mechanical characteristics of NBR and SBR based nanocomposites. Polymer Engineering & Science 2014, 54(4), 942-948.
22. Khalid, M.Y.; Arif, Z.U.; Ahmed, W.; Arshad, H. Recent trends in recycling and reusing techniques of different plastic polymers and their composite materials. Sustainable Materials and Technologies 2022, 31, e00382.
23. El-Nemr, K.F.; Khalil, A.M.; Fathy, E.S. Thermoplastic elastomers based on waste rubber and expanded polystyrene: role of devulcanization and ionizing radiation. International Journal of Polymer Analysis and Characterization 2018, 23(1), 58-69.
24. Manaila, E.; Stelescu, M.D.; Craciun, G.; Surdu, L. Effects of benzoyl peroxide on some properties of composites based on hemp and natural rubber. Polymer bulletin 2014, 71, 2001-2022.
25. Shanmugasundram, H.P.P.V.; Jayamani, E.; Soon, K.H. A comprehensive review on dielectric composites: Classification of dielectric composites. Renewable and Sustainable Energy Reviews 2022, 157, 112075.
26. Aggour, Y.; Al-Shihri, A.; Bazzt, M. Recycling of vulcanized waste rubber through halogenations and amination chemical reactions. WIT Transactions on Ecology and the Environment 2009, 120, 875-883.
27. Sofi, A. Effect of waste tyre rubber on mechanical and durability properties of concrete–A review. Ain Shams Engineering Journal 2018, 9, 2691-2700.
28. Chenrayan, V.; Shahapurkar, K.; Kanaginahal, G.M.; Tirth, V.; Alghtani, A.H.; Algahtani, A.; Ananda Murthy, H.C. Evaluation of dynamic mechanical analysis of crump rubber epoxy composites: experimental and empirical perspective. Journal of the Brazilian Society of Mechanical Sciences and Engineering 2023, 45(3), 145.
29. Araujo-Morera, J.; Hernández Santana, M.; Verdejo, R.; López-Manchado, M.A. Giving a second opportunity to tire waste: An alternative path for the development of sustainable self-healing styrene–butadiene rubber compounds overcoming the magic triangle of tires. Polymers 2019, 11(12), 2122.
30. Chipara, M.; Lozano, K.; Hernandez, A.; Chipara, M. TGA analysis of polypropylene–carbon nanofibers composites. Polymer Degradation and Stability 2008, 93(4), 871-876.
31. Pan, S.; Shuo, L.; Shifeng, W. Interfacial interaction between degraded ground tire rubber and polyethylene. Polymer Degradation and Stability 2017, 143, 85-94.